Articles

Molecular Basis for Interprotein Complex-Dependent Effects on the Redox Properties of Amicyanin†

Zhenyu Zhu,‡ Louise M. Cunane,§ Zhi-wei Chen,§ Rosemary C. E. Durley,§ F. Scott Mathews,*,§ and Victor L. Davidson*,‡

Department of Biochemistry, The University of Mississippi Medical Center, Jackson, Mississippi 39216-4505, and Department of Biochemistry and Molecular Biophysics, Washington University School of Medicine, St. Louis, Missouri 63110

Received July 24, 1998; Revised Manuscript Received September 22, 1998

ABSTRACT: The quinoprotein methylamine dehydrogenase (MADH), type I copper protein amicyanin, and cytochrome *c*-551i form a complex within which interprotein electron transfer occurs. It was known that complex formation significantly lowered the oxidation−reduction midpoint potential (E_m) value of amicyanin, which facilitated an otherwise thermodynamically unfavorable electron transfer to cytochrome *c*-551i. Structural, mutagenesis, and potentiometric studies have elucidated the basis for this complex-dependent change in redox properties. Positively charged amino acid residues on the surface of amicyanin are known to stabilize complex formation with MADH and influence the ionic strength dependence of complex formation via electrostatic interactions. Altering the charges of these residues by site-directed mutagenesis had no effect on the E_m value of amicyanin, ruling out charge neutralization as the basis for the complex-dependent changes in redox properties. The E_m value of free amicyanin varies with pH and exhibits a pK_a value for the reduced form of 7.5. The crystal structure of reduced amicyanin at pH 4.4 reveals that His^{95}, which serves as a ligand for Cu^{2+}, has rotated by 180° about the $C_\beta-C_\gamma$ bond relative to its position in oxidized amicyanin and is no longer in the copper coordination sphere. At pH 7.7, the crystal structure of reduced amicyanin contains an approximately equal distribution of two active-site conformers. One is very similar to the structure of reduced amicyanin at pH 4.4, and the other is very similar to the structure of oxidized amicyanin at pH 4.8. Potentiometric analysis of amicyanin in complex with MADH indicates that its E_m value is not pH-dependent from pH 6.5 to 8.5, and exhibits an E_m value similar to that of free amicyanin at high pH. The structure of reduced amicyanin at pH 4.4, with His^{95} protonated and "flipped", was modeled into the structure of the complex of oxidized amicyanin with MADH. This showed that in the complex, the redox-linked pH-dependent rotation of His^{95} is hindered because it would cause an overlap of van der Waals' radii with residues of MADH. These results demonstrate that protein−protein interactions profoundly affect the redox properties of this type I copper protein by restricting a pH-dependent, redox-linked conformational change of one of the copper ligands.

Methylamine dehydrogenase (MADH)[1] and amicyanin from *Paracoccus denitrificans* form one of the best characterized physiologic electron-transfer complexes of proteins. High-resolution crystal structures are available for the binary complex of MADH and amicyanin (*1*), and a ternary protein complex (*2*) which also includes cytochrome *c*-551i, the electron acceptor for amicyanin. The protein complexes have been shown to be functional in the crystalline state by single-crystal polarized absorption spectroscopy (*3*). The electron-transfer reactions between the tryptophan tryptophylquinone (TTQ) (*4*) prosthetic group of MADH and the type I copper center of amicyanin have been studied in solution by stopped-flow spectroscopy (*5*−*8*). The validity of the protein interface between MADH and amicyanin, which is revealed in the crystal structures, was proven by site-directed mutagenesis of interfacial amino acid residues of amicyanin (*9*).

In *P. denitrificans*, amicyanin is an obligatory mediator of electron transfer from MADH to soluble *c*-type cytochromes (*10*). Each protein is induced in this bacterium during growth on methylamine as a carbon source (*11, 12*). The amicyanin gene is located immediately downstream of that for MADH, and inactivation of the former by gene replacement resulted in loss of the ability to grow on

† This work was supported by NIH Grant GM-41574 (V.L.D.) and NSF Grant MCB-9728885 (F.S.M.).

* Corresponding authors. Victor L. Davidson: Telephone 601-984-1515, fax 601-984-1501, e-mail vdavidson@biochem.umsmed.edu. F. Scott Mathews: telephone 314-362-1080, fax 314-362-7183, e-mail mathews@biochem.wustl.edu.

‡ The University of Mississippi Medical Center.

§ Washington University School of Medicine.

[1] Abbreviations: Ami_{oxi}, oxidized amicyanin; Ami_{red}, reduced amicyanin; BTP, BisTris propane (1,3-bis[tris(hydroxymethylamino)]-propane); E_m, oxidation−reduction midpoint potential; MADH, methylamine dehydrogenase; PMS, phenazine methosulfate; rmsd., root-mean-square deviation; TTQ, tryptophan tryptophylquinone.

10.1021/bi9817919 CCC: $15.00
Published on Web 11/13/1998

methylamine (*13*). MADH, amicyanin, and cytochrome *c*-551i are isolated as individual soluble proteins, but it has been shown that they must form a ternary complex to catalyze methylamine-dependent cytochrome *c*-551i reduction (*10, 14*−*18*). Although it is a thermodynamically favorable reaction, MADH does not reduce cytochrome *c*-551i in the absence of amicyanin (*10*), probably because the proteins are unable to interact in a productive manner. The requirement for amicyanin is quite specific. Other structurally similar type I copper proteins, plastocyanin and azurin, do not effectively substitute for amicyanin (*15, 19*).

At neutral pH, in the absence of MADH, reduced amicyanin is not an effective electron donor for oxidized cytochrome (*17*). This is based on thermodynamic considerations. Redox measurements, which were performed at pH 6.8, yielded oxidation−reduction midpoint potential (E_m) values of +294 mV for amicyanin and +190 mV for cytochrome *c*-551i (14). Thus, electron transfer is highly favored in the reverse of the physiologic direction (i.e., from cytochrome to amicyanin). Under similar reaction conditions, it was shown that the E_m value of amicyanin decreases to +221 mV on complex formation with MADH (*15*). This complex-dependent shift in redox potential is critical as it greatly facilitates the physiologically necessary, but thermodynamically unfavorable, electron-transfer reaction.

The basis for the complex-dependent change in the redox potential of amicyanin has remained a mystery since its initial characterization. We report here that this effect can be largely explained by the fact that complex formation with MADH significantly shifts the pK_a value of reduced amicyanin to much lower pH. Therefore, over the physiologic range of pH, the E_m value of free amicyanin varies with pH, but the E_m value of amicyanin in complex with MADH does not. The reduction of amicyanin is accompanied by a pH-dependent conformational change in which the His^{95} copper ligand rotates when protonated, removing it from the copper coordination sphere. This conformational change, so-called "flipping", is hindered when amicyanin is in complex with MADH. Potentiometric studies, site-directed mutagenesis, and crystallographic analysis are used to characterize this phenomenon and to propose a model that describes the molecular basis for the complex-dependent effects on the redox properties of amicyanin.

EXPERIMENTAL PROCEDURES

Materials. Amicyanin and MADH were purified from *P. denitrificans* (ATCC 13543) as described previously (*11, 20*). The amicyanin mutants, R99D, R99L, K68A, and R99L/K68A, were prepared and purified as described previously (*9*). Completely oxidized forms of amicyanin and MADH were generated by addition of excess potassium ferricyanide. Completely reduced forms of proteins were generated by addition of excess sodium dithionite. Excess reagents were removed by buffer exchange by ultrafiltration using Amicon Centricons. All reagents were purchased from Sigma.

Redox Measurements. The E_m values of amicyanins were determined by spectrochemical titration. The ambient potential was measured directly with a Corning combination redox electrode which was calibrated using quinhydrone (a 1:1 mixture of hydroquinone and benzoquinone) as a standard with an E_m value of +286 mV at pH 7.0 (*21*). Control experiments were performed to determine the E_m values of *N*,*N*,*N*′,*N*′-tetramethyl-*p*-phenylenediamine and 2,6-dichlorophenolindophenol, and results were within 7 mV of literature values.

For measurements of the E_m value of free amicyanin, the reaction mixture contained 20 μM amicyanin in 0.01 M BisTris propane (BTP) buffer at the indicated pH, at 25 °C. Ferricyanide (400 μM) and quinhydrone (200 μM) were present as mediators. The mixture was titrated by addition of incremental amounts of ascorbate, which was used as a reductant, and which had been previously adjusted to the set pH. The reaction was reversible. In the oxidative direction, titration by addition of potassium ferricyanide was performed. The absorption spectrum of amicyanin was recorded at different potentials, and the concentrations of the oxidized amicyanin, [Ami_{oxi}], and reduced amicyanin, [Ami_{red}], were determined by comparison with the spectra of the completely oxidized and reduced forms. E_m values were obtained from plots of potential versus log ([Ami_{oxi}]/[Ami_{red}]).

For measurements of the E_m value of amicyanin in complex with MADH, the reaction mixture contained 20 μM amicyanin and 60−100 μM MADH in 0.01 M BTP, at the indicated pH, at 25 °C. The K_d value for the amicyanin−MADH complex increases with the salt concentration (*22*). In 10 mM buffer at pH 7.5 it is <5 μM. Therefore, under these reaction conditions, complex formation is nearly quantitative. Potassium ferricyanide (400 μM), quinhydrone (200 μM), 1,2-naphthoquinone (100 μM), and phenazine methosulfate (PMS) (40 μM) were present as mediators. The absorption spectrum of the complex was recorded at different potentials, and the concentrations of the oxidized and reduced forms were determined by comparison with the spectra of the completely oxidized complex and a mixture of oxidized MADH with fully reduced amicyanin.

X-ray Data Collection. Crystals of amicyanin were prepared by macroseeding as described previously (*23*). The crystals grew as approximately equidimensional prisms to an average dimension of 0.3−0.4 mm. They are monoclinic, in space group $P2_1$, with unit cell parameters $a = 28.95$ Å, $b = 56.54$ Å, $c = 27.55$ Å, and $\beta = 96.38°$ (*24*). One crystal was transferred to an artificial mother liquor consisting of 3.5 M phosphate buffer (sodium monobasic:potassium dibasic = 9:1), pH ≅ 4.4. Another was transferred to 3.5 M phosphate buffer (sodium monobasic:potassium dibasic = 1:3), pH ≅ 7.7. Prior to data collection, the crystal at pH 4.4 was reduced with 100 mM sodium ascorbate, and the pH 7.7 crystal was reduced with 10 mM ascorbate. In both cases, the dark blue oxidized crystals were rendered colorless within approximately 1 h. X-ray diffraction data were recorded from both crystals to 1.3 Å resolution at room temperature on a Hamlin multiwire area detector (*25*), using graphite-monochromatized X-rays ($\lambda = 1.5418$ Å) produced by a Rigaku RU200 X-ray generator operated at 5 kW. The data were processed using software developed at the University of California at San Diego (*26*). There were no significant changes in cell parameters upon reduction. Data collection statistics and other experimental details are summarized in Table 1.

Refinement of Amicyanin. The refinement of reduced amicyanin was launched with the pH 4.4 data set using, as the initial model, coordinates from oxidized amicyanin

Table 1: Data Collection Statistics for Reduced Amicyanin Crystals

crystal	pH 4.4	pH 7.7
a (Å)	28.96	28.75
b (Å)	56.91	56.20
c (Å)	27.61	27.42
β (deg)	96.81	96.12
R_{Sym}[a] (%)	4.1	5.9
$I/\sigma(I)$[b] (overall)	18.2	13.1
$I/\sigma(I)$ (last shell)[c]	3.8	1.8
completeness (overall) (%)	94	93
completeness (last shell)[c] (%)	71	79
redundancy (overall)	4.9	5.2
redundancy (last shell)[c]	2.1	2.9
$Y/\sigma(Y)$[d] (overall)	33.0	24.8
$Y/\sigma(Y)$ (last shell)[c]	5.3	3.0

[a] $R_{Sym} = \sum_h\sum_i|I(h) - I_i(h)|/\sum_h\sum_i I_i(h)$, where $I_i(h)$ and $I(h)$ are the *i*th and mean measurement of reflection h. [b] $I/\sigma(I)$ is the average signal-to-noise ratio for individual measurements of intensities. [c] The last shell includes the resolution range 1.40−1.30 Å. [d] $Y/\sigma(Y)$ is the average signal-to-noise ratio for merged reflection intensities.

previously refined at 1.3 Å (*24*). All refinements were performed with X-Plor Version 3.843 (*27*). Simulated annealing was employed at the outset to help remove possible structural bias from the starting model (*28*). During simulated annealing, geometric and energetic restraints relating the copper atom to its ligands were applied to maintain stability in the copper site during the molecular dynamics procedure. In all subsequent refinements of the model, the copper−ligand restraints were removed, allowing the copper site to refine freely. Cycles of positional and individual isotropic temperature factor refinement were performed and water molecules were added to the model, using the R_{free} value (*29*) as a guide throughout, with intervening rounds of manual refitting to electron density. Figure 1a shows electron density in the active site. Refinement of amicyanin reduced at pH 7.7 followed the same protocol as that used for reduced amicyanin at low pH, again starting from the oxidized amicyanin coordinates.

In amicyanin reduced at pH 7.7, the $(2F_o - F_c)$ electron density maps showed evidence of disorder in the His^{95} side chain, indicating the possibility of more than one conformer at this pH (Figure 1b). In addition, in both refinements the copper atom displayed slightly aspherical $(2F_o - F_c)$ electron density, more pronounced in the structure at pH 7.7 than in the one at pH 4.4, and small peaks (at the 3σ level) in the $(F_o - F_c)$ residual maps. While such features at the copper atom in general imply anisotropic thermal motion, the apparent disorder in His^{95} suggests that copper also may be adopting different positions in concert with its ligand. Thus, a further refinement of the structure at pH 7.7 was carried out, allowing His^{95} to refine with two alternate conformers and the copper atom to refine over two sites, each with 50% occupancy.

For the purpose of structural comparison between the reduced and oxidized states of amicyanin, oxidized amicyanin was re-refined during this study, using an identical refinement protocol to that used for the reduced proteins, viz., the calculation of R_{free}, use of the Engh and Huber parameter set (*30*) with X-Plor Version 3.843, and the removal of Cu−ligand geometric and energetic restraints. The re-refined structure is essentially identical to the original one (*24*) with an rmsd between the current and previous coordinate sets of 0.06 Å for all 105 C_α atoms. Refinement

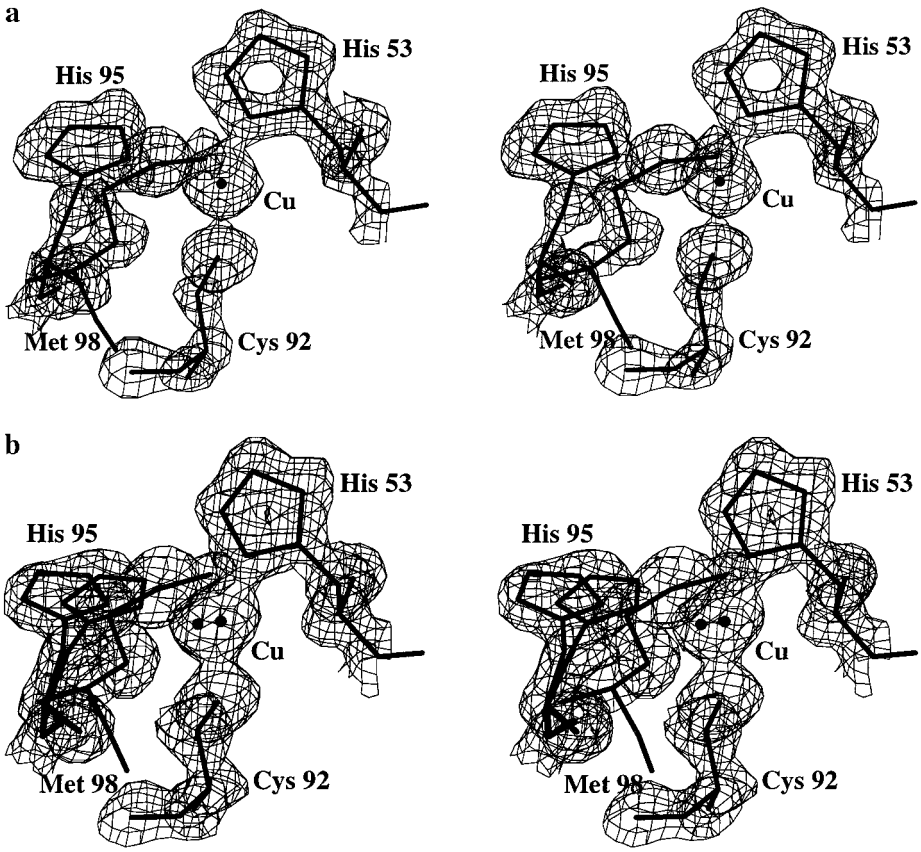

FIGURE 1: $(2F_o - F_c)$ electron density (at 1σ contour level) at the copper site of reduced amicyanin, shown with stick representations of the final refined models. (a) pH 4.4. (b) pH 7.7, illustrating the disordered electron density around His^{95} and aspherical density over copper.

Table 2: Amicyanin Refinement Statistics

	reduced pH 4.4	reduced pH 7.7	reduced pH 7.7 with alternate conformers	oxidized pH 4.8
resolution range (Å)	6.0−1.3	6.0−1.3	6.0−1.3	6.0−1.3
R	0.169	0.182	0.185	0.156
R_{free}	0.195	0.210	0.214	0.180
rmsd bonds (Å)	0.008	0.007	0.007	0.006
rmsd angles (deg)	0.98	0.92	0.97	0.96
no. of solvent molecules	104	97	97	118
average *B* protein (Å^2)	11	14	13	11
average *B* solvent (Å^2)	30	31	34	27
rms Δ*B* bonded atoms (Å^2)				
main chain	1.0	1.3	1.3	0.9
side chain	1.7	2.1	2.2	1.7
% Ramachandran				
most favored	95.5	93.3	93.3	95.5
additional allowed	4.5	6.7	6.7	4.5

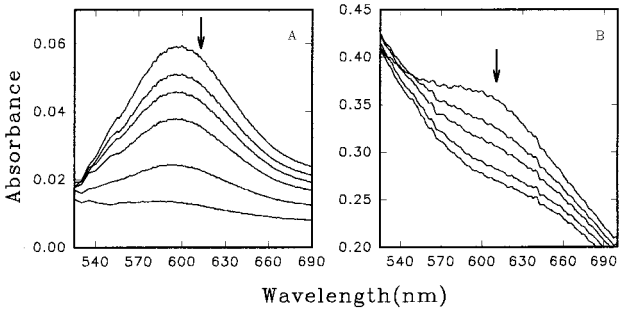

FIGURE 2: Panel A: Reductive titration of oxidized free amicyanin. The sample mixture contained 14 μM amicyanin in the presence of 200 μM quinhydrone and 400 μM ferricyanide, in 10 mM BTP buffer, pH 7.5 at 25 °C. The redox potential was adjusted by addition of ascorbic acid. The curves represent the spectrum of amicyanin at potential values of 302, 287, 269, 261, 250, and 232 mV. The arrow indicates the direction of the absorbance changes with decreasing potential. Panel B: Reductive titration of oxidized amicyanin in complex with MADH. The sample mixture contained 20 μM amicyanin plus 60 μM MADH in the presence of 200 μM quinhydrone, 400 μM ferricyanide, 200 μM 1,2-naphthoquinone, and 40 μM PMS, in 10 mM BTP buffer, pH 7.5 at 25 °C. The redox potential was adjusted by addition of ascorbic acid. The curves represent the spectrum of amicyanin at potential values of 312, 253, 220, 196, and 186 mV. The arrow indicates the direction of the absorbance changes with decreasing potential.

statistics for the two reduced amicyanin structures, the reduced amicyanin at pH 7.7 with alternate conformers, and the oxidized amicyanin are summarized in Table 2.

RESULTS

pH Dependence of E_m Values. The redox potentials of amicyanin free and in complex with MADH were measured over a range of pH values. Representative examples of redox titrations of these two forms are shown in Figure 2. The E_m values of both forms of amicyanin were obtained by plotting the ambient potential versus log ([Ami_{oxi}]/[Ami_{red}]), and fitting the data to the Nernst equation:

$$E = E_m + (2.3RT/nF) \log ([Ami_{oxi}]/[Ami_{red}]) \quad (1)$$

A linear relationship was obtained at each pH over the range that was studied (data not shown). Slopes of the fitted lines at different pH values ranged from 0.9 to 1.1, which is consistent with the one-electron redox reaction of the Cu^{2+}/Cu^{+} redox couple of amicyanin. The error in the fitted E_m value was typically within ±7 mV. For measurements of amicyanin in complex with MADH at pH >8, the error was ±12 mV because the stability of the mediator PMS decreased at the higher pH values.

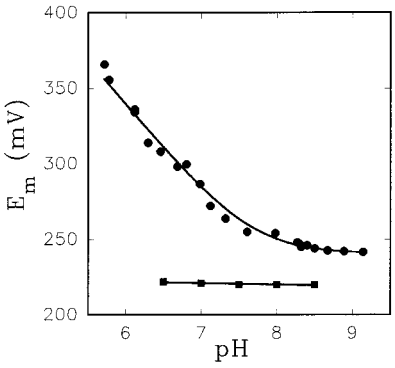

FIGURE 3: Dependence on pH of the E_m values of amicyanin free and in complex with MADH. The E_m values of amicyanin free (●) and in complex with MADH (■) were determined in 10 mM BTP buffer, at 25 °C at the indicated pH. The curve represents the fit of the data for free amicyanin to eq 2.

The pH dependencies of the E_m values of amicyanin free and in complex with MADH were dramatically different. The redox potential of free amicyanin exhibited a clear dependence on pH, whereas the E_m value of amicyanin in complex was essentially independent of pH (Figure 3). The dependence of the E_m value of free amicyanin on pH is characteristic of a single protonated ligand, and the data are well fit by eq 2:

$$E_m = E_{m,7} - 59.3 \log\left(\frac{10^{-7} + K_a}{[H^+] + K_a}\right) \quad (2)$$

The fit yielded a pK_a value of 7.5 ± 0.3. The E_m value at high pH plateaus at 240 ± 7 mV. The redox potential of amicyanin, when in complex with MADH, is essentially independent of pH over the same range. An E_m value of 220 ± 10 mV is obtained. Measurements could not be made over as wide a range of pH with the complex because of pH-dependent perturbations of the absorption spectrum of MADH which interfered with the analysis, and instability of MADH at the more extreme values of pH over the relatively long time course of these redox titrations (>1 h).

These results are consistent with the previously reported E_m value of free amicyanin of 294 mV at pH 6.8 (*14*), and the complex-dependent decrease in the E_m value of amicyanin of 73 mV at pH 7.0 (*15*). It is clear from the results in Figure 3 that the magnitude of the complex-dependent change in the redox potential of amicyanin depends on the pH. It increases with decreasing pH because the potential of free amicyanin increases with decreasing pH, while that of amicyanin in complex remains constant. Extrapolation of the two curves in Figure 3 to infinite pH indicates that in the high-pH region, where the ionization of amicyanin is no longer a factor, a residual pH-independent complex-dependent ΔE_m of 20 ± 12 mV remains.

Effect of Surface Charge on the E_m Value of Amicyanin. The crystal structure of the MADH−amicyanin complex reveals that the interaction of the two proteins is stabilized by an interprotein salt bridge involving Arg^{99} of amicyanin. A second weaker ionic interaction involving Lys^{68} may also

Table 3: Redox Potentials of Mutant Amicyanins

amicyanin	E_m value (mV)[a]
wild-type	266 ± 7
R99D	263 ± 6
R99L	258 ± 7
K68A	275 ± 8
R99L/K68A	264 ± 7
F97E	263 ± 8

[a] Values represent the average of 3−7 sets of measurements ± the standard deviation.

be inferred from the structure. Site-directed mutagenesis studies have confirmed the importance of ionic interactions of Arg[99] in stabilizing complex formation (*9*). These results raise the possibility that neutralization of the positive charges on Arg[99] or Lys[68] could be responsible for the observed complex-dependent decrease in the E_m value of amicyanin. To test this hypothesis, the E_m values of site-directed mutants of amicyanin were determined and compared with that of the wild-type (Table 3). Three single mutations, R99D, R99L, and K68A, and a double mutant, R99L/K68A, were examined. The E_m values of the mutants and wild type were essentially indistinguishable. Furthermore, mutation of Phe[97], which resides in the hydrophobic patch on the surface of amicyanin near the copper site, to Glu also has no significant effect on the E_m value of amicyanin (*31*). Thus, the complex-dependent changes in the redox potential of amicyanin cannot be attributed to the neutralization of positive surface charges on amicyanin near the copper site which occurs on complex formation. In fact, this demonstrates that the E_m value of amicyanin is relatively insensitive to changes in surface charge in the vicinity of the type I copper site.

pH- and Redox-Dependent Structural Changes in Amicyanin. The overall structures of reduced amicyanin at pH 4.4 and pH 7.7 are essentially identical to the oxidized amicyanin structure that was determined at pH 4.8. The short loop formed by residues 17−20 shows some conformational variability among the three structures (oxidized and two reduced), which is not unexpected as this segment of the protein exhibited poor electron density and high temperature factors in all the refinements. The significant differences between the oxidized and reduced states of amicyanin are confined to the type I copper site. Figure 4 shows the structure of the copper site of reduced amicyanin at pH 4.4 superimposed on that of oxidized amicyanin. Table 4 compares the Cu−ligand distances in reduced amicyanin at pH 4.4 and 7.7, and in oxidized amicyanin.

In amicyanin reduced at pH 4.4, the ligand His[95] has dissociated from copper after protonation of the $N^{\delta 1}$ atom and rotated by 180° about the $C_\beta-C_\gamma$ bond, a phenomenon coined the histidine flip. The flip is inferred in part from the arrangement of ordered water molecules in the immediate vicinity of the His[95] side chain. In the oxidized amicyanin structure, a water molecule (Wat1) forms a bridging hydrogen bond between His[95]($N^{\epsilon 2}$) and the backbone of a symmetry-related protein molecule, and makes another hydrogen bond with an adjacent water molecule (Wat2). In reduced amicyanin at pH 4.4, Wat1 and Wat2 are present in nearly identical positions, but His[95]($N^{\epsilon 2}$) now makes a hydrogen bond to Wat2 instead of Wat1, and a new hydrogen bond is formed between His[95]($N^{\delta 1}$) and a new water molecule (Wat3). This is possible only if the His[95] side chain has rotated about the $C_\beta-C_\gamma$ bond. Accordingly, His[95] was modeled in the flipped orientation for the final cycles of refinement. The position of Cu(I) differs by about 0.6 Å from that of Cu(II) in oxidized amicyanin, where its coordination adopts a distorted tetrahedral configuration. On reduction, Cu(I) has moved into the plane of His[53]($N^{\delta 1}$)−Cys[92](S^γ)−Met[98](S^δ). This results in trigonal planar coordination for Cu(I), its preferred ligand arrangement. These three copper ligands of the reduced structure have very similar orientations to those of their counterparts in oxidized amicyanin.

In amicyanin reduced at pH 7.7, the His[95] ligand had *apparently* also dissociated from the copper, and therefore was modeled with the flipped orientation as in the pH 4.4 structure. The Cu−His[95] distance is slightly shorter than at pH 4.4 (see Table 4), and the copper atom sits in a similar location to that in the low-pH structure, about 0.5 Å from the oxidized copper position, close to the N−S−S′ plane. In the high-pH reduced amicyanin, the conserved water molecules adjacent to His[95] (Wat1 and Wat2) have high temperature factors and weak, disordered electron density. Also, there is no water observed in the Wat3 position. Therefore, the status of His[95] flipping is less certain at pH 7.7. It may, however, be resolved from the results of the redox experiments that have determined that free amicyanin has a pK_a value of approximately 7.5 (Figure 3). If one attributes this to the protonation of the His[95] ligand, then in crystals of amicyanin reduced at pH 7.7 it is likely that an equilibrium mixture of doubly protonated "flipped" and singly protonated "nonflipped" His[95] exists. This would account for the observed ill-defined solvent structure adjacent to the histidine. To reflect this possibility, we subsequently refined the active site (as discussed earlier under Experimental Procedures) with alternate sites for the copper atom, and alternate conformers of His[95] representing this equilibrium mixture. His[95] refined successfully into two discrete side-chain conformers, and Cu occupies two sites about 0.7 Å apart (Figure 1b). The resultant Cu−ligand distances for conformers A and B are included in Table 4. When the active sites of oxidized amicyanin, reduced amicyanin at pH 4.4, and reduced amicyanin at pH 7.7 with alternate conformers are superimposed, conformation A is very similar to that of the oxidized structure and conformation B to the reduced structure at pH 4.4. This strongly suggests that at pH 7.7 the reduced copper site is comprised of an equilibrium mixture of two conformational states, one with an oxidized-like pseudotetrahedral geometry (i.e., His[95] singly protonated) and the other with the low-pH-reduced trigonal planar arrangement (i.e., His[95] doubly protonated).

Another difference between the oxidized and reduced states observed in the vicinity of the copper site is a lengthening of the hydrogen bond between the S^γ atom of the Cys[92] ligand and the amide N of Asn[54], from 3.6 Å in the oxidized to 3.8 Å in the reduced structures. This N−H···S hydrogen bond to the cysteine ligand is characteristic of blue copper sites (*32*). This may be significant since small differences in hydrogen bonding networks in or near the copper site have been postulated to influence the electronic properties of cupredoxins (*33*).

DISCUSSION

Complex-Dependent Changes in the Redox Properties of Amicyanin. The present studies show that the pH dependence

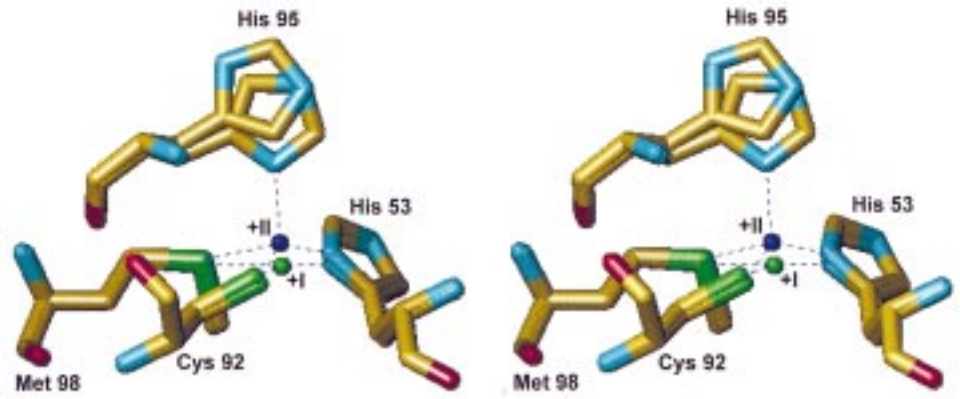

FIGURE 4: Comparison of the active site structures of reduced amicyanin at pH 4.4 and of oxidized amicyanin at pH 4.8. Atom types are indicated by color: carbon, yellow; nitrogen, aqua; oxygen, red; sulfur, green; copper(II), dark blue; copper(I), green. In the oxidized structure, the copper(II) has four ligands, and in the reduced structure the copper(I) has three ligands.

Table 4: Copper−Ligand Distances in Oxidized and Reduced Amicyanins

			reduced pH 7.7[a]		
				alternate conformers	
distances (Å)	oxidized pH 4.8	reduced pH 4.4	full occupancy	A	B
Cu−His53($N^{\delta 1}$)	1.96	1.91	1.90	2.18	1.83
Cu−Cys92(S^{γ})	2.08	2.09	2.12	2.09	2.15
Cu−His95($N^{\delta 1}$/$C^{\delta 2}$)	2.03	3.51	3.43	2.07	3.92
Cu-Met98(S^{δ})	2.91	2.90	2.91	3.00	2.88

[a] As discussed in the text, in addition to a refinement with all atoms refined at full occupancy, the reduced amicyanin at pH 7.7 was refined with two partially occupied (50%) copper positions and alternate conformers of His^{95}; one singly protonated and not "flipped" (A), the other doubly protonated and "flipped" (B).

of the E_m value of amicyanin free in solution correlates with that of a single protonated ligand having a pK_a of 7.5. The crystal structures of oxidized amicyanin at pH 4.8 and reduced amicyanin at pH 4.4 show that the His^{95} copper ligand is doubly protonated in the reduced and singly protonated in the oxidized states, and undergoes a conformational change between the two states. At pH 7.7, the conformation of His^{95} in the reduced crystal appears to be that of an equilibrium mixture of the two states, as one would expect at a pH value near the pK_a for this transition. We conclude that the protonation of His^{95}, that is linked to the reduction of copper and to the conformational change of this residue, is responsible for the pH dependence of the E_m value. Further support for this idea may be inferred from studies of amicyanin from *Thiobacillus versutus*. It was shown that the NMR chemical shift of the C_2H proton of a histidine copper ligand was pH-dependent and titrated with a pK_a of 7.4 at 25 °C (*34*). EXAFS analysis of the *T. versutus* protein also indicated that one of the Cu−N interactions in reduced amicyanin is lost at low pH (*35*). Thus, what we observed in the crystal structures appears to accurately reflect the conformations of the protein in solution, and directly relates to the results of the potentiometric analyses.

In an effort to understand from a structural perspective why the redox potential of amicyanin in complex with MADH is *not* pH-dependent over the range of pH studied while that of free amicyanin is, the crystal structure of reduced free amicyanin at low pH was modeled into the 1.9 Å structure of the MADH−amicyanin−cytochrome *c*-551i complex[2] (Figure 5). This was accomplished using computer graphics to map the C_α atoms of reduced free amicyanin onto those of the amicyanin in complex using a least-squares fit (*36*). This model clearly demonstrates that the observed pH-dependent conformational change of His^{95} in reduced free amicyanin would be sterically hindered at the interface between amicyanin and MADH because of overlap between the His^{95} side chain of amicyanin and the aliphatic part of the Glu^{101} side chain of the L-subunit of MADH (Figure 5). Thus, in the complex His^{95} is prevented from dissociating from the copper coordination sphere upon reduction, and the redox potential of amicyanin in complex remains similar to that of free amicyanin at the highest values of pH, where it is singly protonated and unflipped.

A small residual difference in the E_m value of about 20 mV was observed (Figure 3) at high pH between amicyanin in complex and free, where the redox potential of free amicyanin is no longer pH-dependent. A comparison of crystalline oxidized amicyanin alone and within the complex reveals some small differences in and near the copper site (Table 5) which may be responsible for this pH-independent difference in E_m value. The His^{95} ligand adopts a slightly different conformation in the complex,[2] in both its side chain and its backbone. The copper atom also takes up a different position in the complex, about 0.3 Å away from that in free amicyanin. The relative positions of Cu and ligands in the complex result in significant differences in the Cu−Cys^{92}(S^{γ}) and Cu−Met^{98}(S^{δ}) distances compared with those in free amicyanin (Table 5). It is possible that modification of these Cu−ligand bonds on complex formation could be responsible for fine-tuning the redox potential of amicyanin (*37*).

Relationship to Other Blue Copper Proteins. Amicyanins are members of a class of copper proteins referred to as type I copper proteins, blue copper proteins, or cupredoxins (*32*). Of the subclasses of blue copper proteins, amicyanin shows the strongest sequence and structural similarities to the plastocyanins (*38, 39*). It is noteworthy that the reduced forms of plastocyanin and pseudoazurin also display a histidine flip at low pH. Amicyanin, plastocyanin and pseudoazurin are similar in that they have very short amino acid spacings between the three C-terminal active site

[2] R. C. E. Durley, Z. Chen, F. S. Mathews, unpublished results.

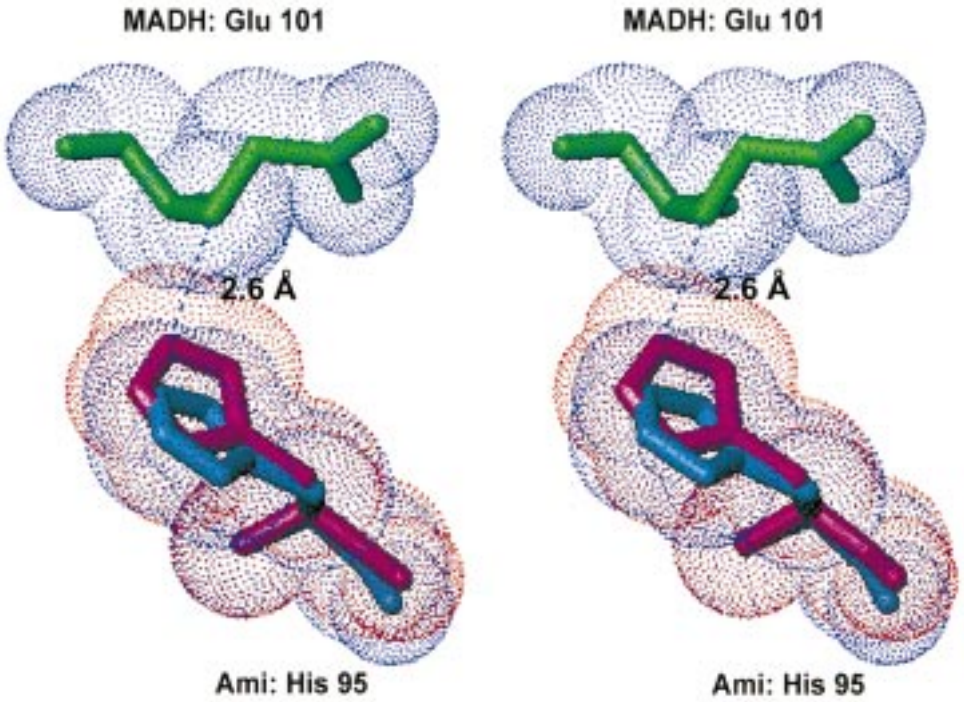

FIGURE 5: Stereoview of the flipped His^{95} of reduced amicyanin modeled into the 1.9 Å structure of the MADH−amicyanin−cytochrome *c*-551i complex. van der Waals' dot surfaces are drawn in red for the reduced amicyanin and in blue for the amicyanin and MADH L-subunit in the complex.

Table 5: Copper−Ligand Distances in Oxidized Amicyanin, Free and in Complex with MADH and Cytochrome *c*-551i

distances (Å)	free amicyanin	amicyanin in complex[a]
Cu−His53($N^{\delta 1}$)	1.96	1.98 ± 0.05
Cu−Cys92(S^{γ})	2.08	2.25 ± 0.04
Cu−His95($N^{\delta 1}$)	2.03	1.98 ± 0.05
Cu-Met98(S^{δ})	2.91	2.71 ± 0.02

[a] Distances were averaged over four amicyanin molecules per asymmetric unit with the estimated standard deviations indicated.

residues compared with other cupredoxins (*40*−*42*). In the crystallographic study of reduced plastocyanin (*43*), the structures at six pH values, in the range 3.8−7.8, were determined. As seen in amicyanin at pH 4.4, the low-pH plastocyanin structure (pH 3.8) indicates that the C-terminal histidine ligand has dissociated from the metal, and Cu(I) has moved into the N−S−S′ plane of the three remaining ligands, resulting in trigonal planar coordination. In the high-pH form of plastocyanin (pH 7.8), the active site was very similar to that of oxidized plastocyanin. The copper site structures at intervening pH values were interpreted as weighted averages of the low-pH and high-pH forms, and as a reflection of dynamic equilibrium between the two forms in solution. The pK_a for the conformational change of the C-terminal histidine ligand, as inferred from the crystallographic study (*43*), as well as the pK_a for the pH dependence of the redox potential of plastocyanin (*44*) are much lower (i.e., 5.9) than that reported here for free amicyanin. This may be relevant to the respective physiologic functions of plastocyanin and amicyanin. Plastocyanin resides in the intrathylakoid space which is acidic, and is believed to be ≤pH 5 (*45*). Amicyanin functions in the periplasmic space, the pH of which is unknown. Since the bacterial outer membrane is relatively permeable to small solutes, it is usually assumed that the pH of the periplasm will approximate that of the external medium. Thus, the respective pK_a values for the histidine flip and redox potential for plastocyanin and amicyanin appear to be in the range of their respective physiologic pH values.

Pseudoazurin, another blue copper protein, undergoes pH-dependent protonation and dissociation of the C-terminal histidine ligand in the reduced form, with a pK_a of about 4.7 (*40*). Kinetic and NMR data for pseudoazurin from *Achromobacter cycloclastes* (*40*) are consistent with reversible protonation of this ligand. A crystallographic study (*46*) of reduced pseudoazurin from *Alcaligenes faecalis* at pH 4.4 and 7.8 found that the histidine ligand dissociated from copper at the lower pH, leading to trigonal planar copper coordination, while at the higher pH the active site was similar to that of oxidized pseudoazurin.

Relevance of Complex-Dependent Redox Properties to Binding. Since complex formation with MADH changes the redox potential of amicyanin under physiologic conditions, it follows that the oxidized and reduced forms of amicyanin will exhibit different binding constants for the association with MADH under these conditions. The relationship between the redox potentials of amicyanin free and bound to MADH and the dissociation constants for the complexes of oxidized and reduced amicyanin may be described by eq 3:

$$E_m(\text{free}) - E_m(\text{bound}) = (59.3\ \text{mV})\log\,[K_d(\text{red})/K_d(\text{ox})] \quad (3)$$

This relationship predicts that at pH 7, oxidized amicyanin will have approximately a 5-fold greater affinity for MADH than will reduced amicyanin. This difference in affinity will increase as pH decreases. The results of kinetic studies with metal-substituted *T. versutus* amicyanin support the conclusion that MADH has a higher affinity for oxidized amicyanin than for reduced amicyanin (*47*).

Scheme 1

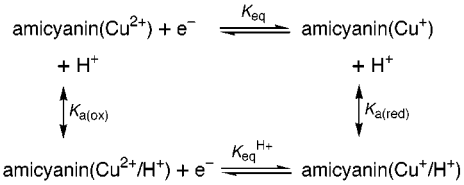

The values of K_d, pK_a, and E_m are interrelated. The relationship between the pK_a and E_m values may be described according to Scheme 1, where K_a(ox) and K_a(red) are the acid dissociation constants for the two redox forms of amicyanin. K_{eq} and K_{eq}^{H+} are related to the E_m values for the unprotonated and protonated forms of amicyanin, respectively, according to eq 1. The pK_a value determined from the data in Figure 3 is that of reduced amicyanin. The pK_a value for the oxidized protein would be much lower than the lowest pH in this study. Thus, the His^{95} copper ligand on the oxidized amicyanin will always be unprotonated in the pH range that was studied. A critical point is that upon complex formation with MADH, the amicyanin(Cu^+/H^+) state is not allowed for steric reasons (see Figure 5). Therefore, in the presence of MADH, the equilibrium between amicyanin(Cu^+) and amicyanin(Cu^+/H^+) is shifted to favor the unprotonated state. From the titration data in Figure 3, it can be seen that the shift in equilibrium has lowered the pK_a(red) to a value below the pH range studied. As such, the E_m values measured in the presence of MADH are not dependent on pH over the range of pH 6.5−8.5 and are comparable to the E_m value in the absence of MADH at high pH.

It has been reported (*48*) that plastocyanin also exhibits a complex-dependent change in redox potential when it binds to photosystem I, its physiologic electron acceptor. In contrast to what was observed with amicyanin and MADH, the E_m value of plastocyanin became more positive by 50−60 mV on complex formation. The difference in the direction of the change in redox potential is consistent with the physiologic functions of the two copper proteins. Amicyanin is the electron acceptor for MADH, so it is reasonable that the reduced form of the enzyme should exhibit less affinity than the oxidized form. Plastocyanin is the electron donor for photosystem I, and the opposite direction of the complex-dependent change in redox potential means that the reduced form of plastocyanin will exhibit a greater affinity than the oxidized form.

Relationship to Other Redox Protein Complexes. Other examples of redox potentials of protein-bound redox centers that are sensitive to protein−protein interactions have been reported. These include the following. The E_m value of the cytochrome *c* subunit of *p*-cresol methylhydroxylase increases by 60−70 mV on association with its flavin subunit to form the holoenzyme (*49*). The E_m value of the hydroxylase component of the methane monooxygenase complex increases by 104 mV on association with the reductase component (*50*). The E_m value of the iron protein of the nitrogenase complex decreases by 200 mV on association with the molybdenum−iron protein (*51*). The E_m values of ferredoxin and ferredoxin−$NADP^+$ oxidoreductase each change on complex formation with each other (*52*). The change in the E_m value of plastocyanin on association with photosystem I (*48*) was discussed earlier. In the case of nitrogenase, it appears that the change in redox potential may be explained by changes in solvent accessibility and the protein environment of the redox center which accompany complex formation (*51*). Beyond that, and the results presented here, there is little understanding of the basis for such changes in redox potential caused by protein−protein interaction.

The types of redox measurements described above have not routinely been made with redox proteins, and rarely have such complex-dependent changes in redox potential been examined as a function of reaction conditions such as pH. It may be that changes in redox potential caused by protein−protein interactions are a relatively common phenomenon. In this study we have described the structural basis for a change in redox potential, that is coupled to an ionization event, which is in turn coupled to a significant conformational change of the redox center. By restricting the ability of that conformational change to occur, the protein−protein interaction has profoundly modified the redox properties of amicyanin. Thus, in this case it has been possible to determine the structural and molecular basis for the complex-dependent change in redox properties.

REFERENCES

1. Chen, L., Durley, R., Poloks, B. J., Hamada, K., Chen, Z., Mathews, F. S., Davidson, V. L., Satow, Y., Huizinga, E., Vellieux, F. M. D., and Hol, W. G. J. (1992) *Biochemistry 31*, 4959−4964.
2. Chen, L., Durley, R., Mathews, F. S., and Davidson, V. L. (1994) *Science 264*, 86−90.
3. Merli, A., Brodersen, D. E., Morini, B., Chen, Z., Durley, R. C. E., Mathews, F. S., Davidson, V. L., and Rossi, G. L. (1996) *J. Biol. Chem. 271*, 9177−9180.
4. McIntire, W. S., Wemmer, D. E., Christoserdov, A. Y., and Lindstrom, M. E. (1991) *Science 252*, 817−824.
5. Brooks, H. B., and Davidson, V. L. (1994) *J. Am. Chem. Soc. 116*, 11201−11202.
6. Brooks, H. B., and Davidson, V. L. (1994) *Biochemistry 33*, 5696−5701.
7. Bishop, G. R., and Davidson, V. L. (1995) *Biochemistry 34*, 12082−12086.
8. Bishop, G. R., and Davidson, V. L. (1997) *Biochemistry 36*, 13586−13592.
9. Davidson, V. L., Jones, L. H., Graichen, M. E., Mathews , F. S., and Hosler, J. P. (1997) *Biochemistry 36*, 12733−12738.
10. Husain, M., and Davidson, V. L. (1986) *J. Biol. Chem. 261*, 8577−8580.
11. Husain, M., and Davidson, V. L. (1985) *J. Biol. Chem. 260*, 14626−14629.
12. Husain, M., and Davidson, V. L. (1987) *J. Bacteriol. 169*, 1712−1717.
13. van Spanning, R. J. M., Wansell, C. W., Reijnders, W. N. M., Oltmann, L. F., and Stouthamer, A. H. (1990) *FEBS Lett. 275*, 217−220.
14. Gray, K. A., Knaff, D. B., Husain, M., and Davidson, V. L. (1986) *FEBS Lett. 207*, 239−242.
15. Gray, K. A., Davidson, V. L., and Knaff, D. B. (1988) *J. Biol. Chem. 263*, 13987−13990.
16. Davidson, V. L., and Jones, L. H. (1991) *Anal. Chim. Acta 249*, 235−240.
17. Davidson, V. L., and Jones, L. H. (1995) *J. Biol. Chem. 270*, 23941−23943.
18. Davidson, V. L., and Jones, L. H. (1996) *Biochemistry 35*, 8120−8125.
19. Hyun, Y.-L., and Davidson V. L. (1995) *Biochemistry 34*, 12249−12254.
20. Davidson, V. L. (1990) *Methods Enzymol. 188*, 241−246.

21. Cammack, R. (1995) in *Bioenergetics: A Practical Approach* (Brown, G. C., and Cooper, C. E., Eds.) pp 85−109, IRL Press, New York.
22. Davidson, V. L., Graichen, M. E., and Jones, L. H. (1993) *Biochim. Biophys. Acta 1144*, 39−45.
23. Lim, L. W., Mathews, F. S., Husain, M., and Davidson, V. L. (1986) *J. Mol. Biol. 189*, 257−258.
24. Cunane, L. M., Chen, Z.-W., Durley, R. C. E., and Mathews, F. S. (1996) *Acta Crystallogr. D52*, 676−686.
25. Hamlin, R. (1985) *Methods Enzymol. 114*, 416−452.
26. Howard A. J., Nielsen C., and Xuong N. H. (1985). *Methods Enzymol. 114*, 452−472.
27. Brünger, A. T. (1992) X-PLOR version 3.1. *A system for crystallography and NMR*, Yale University Press, New Haven.
28. Hodel, A., Kim, S.-H., and Brünger, A. T. (1992) *Acta Crystallogr. A48*, 851−858.
29. Brünger, A. T. (1992) *Nature 355*, 472−475.
30. Engh, R. A., and Huber, R. (1991) *Acta Crystallogr. A47*, 392−400.
31. Davidson, V. L., Jones, L. H., and Zhu, Z. (1998) *Biochemistry 37*, 7371−7377.
32. Adman, E. T. (1991) *Adv. Protein Chem. 42*, 145−197.
33. Adman, E. T., Turley, S., Bramson, R., Petratos, K., Banner, D., Tsernoglou, D., Beppu, T., and Watanabe, H. (1989) *J. Biol. Chem. 264*, 87−99.
34. Lommen, A., and Canters, G. W. (1990) *J. Biol. Chem. 265*, 2768−2774.
35. Lommen, A., Pandya, K. I., Koniingsberger, D. C., and Canters, G. W. (1991) *Biochim. Biophys. Acta 1076*, 439−447.
36. Rao, S. T., and Rossmann, M. G. (1973) *J. Mol. Biol. 76*, 241−256.
37. Guckert, J. A., Lowery, M. D., and Solomon, E. I. (1995) *J. Am. Chem. Soc. 117*, 2817−2844.
38. Durley, R., Chen, L., Lim, L. W., Mathews, F. S., and Davidson, V. L. (1993) *Protein Sci. 2*, 739−752.
39. van Beeumen, J., van Bun, S., Canters, G. W., Lommen, A., and Chothia, C. (1991) *J. Biol. Chem. 266*, 4869−4877.
40. Dennison, C., Kohzuma, T., McFarlane, W., Suzuki, S., and Sykes, A. G. (1994) *J. Chem. Soc., Chem. Commun*., 581−582.
41. Guss, J. M., Merritt, E. A., Phizackerley, R. P., and Freeman, H. C. (1996) *J. Mol. Biol. 262*, 686−705.
42. Kyritsis, P., Dennison, C., Kalverda, A. P., Canters, G. W., and Sykes, A. G. (1994) *J. Chem. Soc., Dalton Trans. 20*, 3017−3023.
43. Guss, J. M., Harrowell, P. R., Murata, M., Norris, V. A., and Freeman, H. C. (1986) *J. Mol. Biol. 192*, 361−387.
44. Segal, M. G., and Sykes, A. G. (1978) *J. Am. Chem. Soc. 100*, 4585−4592.
45. Gross, E. L. (1993) *Photosynth. Res. 37*, 103−116.
46. Vakoufari, E., Wilson, K. S., and Petratos, K. (1994) *FEBS Lett. 347*, 203−206.
47. Ubbink, M., Hunt, N. I., Hill, H. A. O., and Canters, G. W. (1994) *Eur. J. Biochem. 222*, 561−571.
48. Drepper, F., Hippler, M., Nitschke, W., and Haehnel, W. (1996) *Biochemistry 35*, 1282−1295.
49. Hopper, D. J. (1983) *FEBS Lett. 161*, 100−102.
50. Lui, Y., Nesheim, J. C., Paulsen, K. E., Stankovich, M. T., and Lipscomb, J. D. (1997) *Biochemistry 36*, 5223−5233.
51. Lanzilotta, W. N., and Seefeldt, L. C. (1997) *Biochemistry 36*, 12976−12983.
52. Smith, J. M., Smith, W. H., and Knaff, D. B. (1981) *Biochim. Biophys. Acta 635*, 405−411.

BI9817919